Mechanical Effects on the Electronic Properties of a Biphenyl-Based Molecular Switch

ARTICLE *in* THE JOURNAL OF PHYSICAL CHEMISTRY C · FEBRUARY 2015

Impact Factor: 4.77 · DOI: 10.1021/jp510697a

3 AUTHORS:

Martin Eduardo Zoloff Michoff

National University of Cordoba, Argentina

21 PUBLICATIONS **104** CITATIONS

SEE PROFILE

Ezequiel Castillo

National University of Cordoba, Argentina

2 PUBLICATIONS **3** CITATIONS

SEE PROFILE

Ezequiel Pedro Marcos Leiva

National University of Cordoba, Argentina

182 PUBLICATIONS **2,004** CITATIONS

SEE PROFILE

THE JOURNAL OF PHYSICAL CHEMISTRY C

Article

pubs.acs.org/JPCC

Mechanical Effects on the Electronic Properties of a Biphenyl-Based Molecular Switch

Martin E. Zoloff Michoff,*[,†,‡] M. Ezequiel Castillo,[†] and Ezequiel P. M. Leiva[†]

[†]INFIQC, CONICET and Departamento de Matemática y Física, Facultad de Ciencias Químicas, Universidad Nacional de Córdoba, Córdoba, Argentina

Supporting Information

ABSTRACT: Using a combination of density functional theory and nonequilibrium Green's function calculations, the effect of mechanically stretching a biphenyl-based molecular switch bonded to Au electrodes was studied. Thermodynamic and transport properties of the high- and low-conductance species were analyzed. A disulfide functionality bridging the aromatic rings was used to switch between the high- and low-conductance species. The potential of such a system as a molecular device has already been confirmed (*J. Phys. Chem. C* **2013**, *117*, 25724). Mechanically stretching the molecular junction has major effects on both the thermodynamics of the switching reaction and the conductance ratio between the high- and low-conductance species involved in the molecular switch. It is also shown that the conductance of each individual species can be modulated by means of an external mechanical force, thus providing a dual switching mechanism for the proposed system.

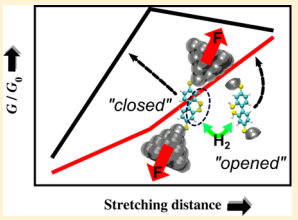

INTRODUCTION

Molecular electronics is a fast-growing field that is fueled by the advent of novel and powerful experimental techniques[1−10] that allow single-molecule junctions to be built and studied. Modern computational tools have also proved to be of great value, not only in obtaining insight at the nanoscale level but also in allowing an understanding of the properties of these systems at a fundamental level.[9,11−13]

One of the aspects that is of great importance for the effective design of these types of devices at the nanoscale is the consideration of the mechanical properties of such molecule/metal interfaces.[14−23] An external stress not only affects the temporal stability of the molecular junction, but it can also allow for the control of its properties. For instance, in a recent computational work, a mechanically activated molecular switch was proposed.[24,25] Molecular dynamics simulations were carried out to study how a conductive atomic force microscope tip could be used to reversibly unfold and refold a π-stack with a concomitant conductance change. In another recent ab initio molecular dynamics study, it was shown that the conductance of a simple molecular junction can be modulated by means of a mechanical force.[26] The effects of mechanical stress on the transport properties of polymers,[27] alkanedithiols,[28,29] alkanediamines,[29] 4,4′-bipyridine,[30] and DNA[31] have also been reported.

Biphenyldithiol has attracted considerable interest as a model compound for a molecular switch. The transport properties in this system depend on the torsion angle between the aromatic rings. This has been confirmed experimentally[32−34] and theoretically.[35−37] Using a biphenyldithiol/Au molecular junction as a model, it was recently suggested that the combination of mechanical pulling and optical control can be used to enhance the electron-transport properties of such systems.[38]

In a recent computational study, we demonstrated the potential of a biphenyl system with a disulfide functionality bridging the aromatic rings as a (electro)chemically triggered molecular switch.[39] The electron-transport properties of this molecular system attached on either extreme to gold clusters, which mimicked the tips of two electrodes, by means of a S−Au bond were evaluated. It was shown that the torsion angle, and, in turn, the transport properties of the molecular junction, can be controlled by reducing/oxidizing the disulfide functionality, allowing the system to switch between a "closed" (high-conductance) and an "opened" (low-conductance) species. Moreover, the reduction of the anchoring sulfur atoms was also considered as a possible side reaction. Our calculations demonstrated that this unwanted reaction is less favorable by ∼0.6 eV and, thus, would not compete with the switching reaction under certain conditions.

In the current work, we now focus on the effects of mechanically stretching a metal/molecule nanojunction on these two key aspects of the proposed molecular switch: the thermodynamics of the switching reaction and the competing reaction and the transport properties of the species involved. We show that mechanical stress has a major impact on both of these issues.

When the nanojunction is highly stressed, the energy difference between the reduction reactions on the disulfide functionality and on the anchoring groups is decreased from ∼0.6 to ∼0.3 eV, that is, the undesired side product becomes relatively more favorable. Nonetheless, the reduction of the disulfide bridge remains the most stable product throughout the stretching pathway from a thermodynamic point of view.

Received: October 24, 2014
Revised: February 9, 2015

DOI: 10.1021/jp510697a
J. Phys. Chem. C XXXX, XXX, XXX−XXX

Scheme 1. Structures of Au−S−Ox, Au−S−Red, and Au−SH−Ox[a]

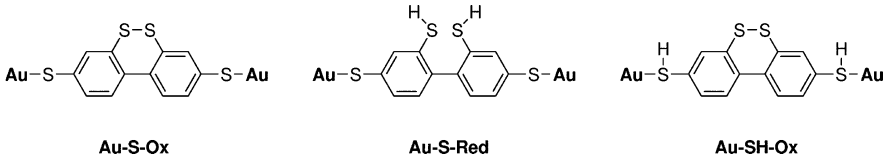

[a]Note that the Au atom is intended only as a schematic representation of the gold tip.

Regarding the electron-transport properties of the species involved in the molecular switch, the absolute conductance of both closed and opened species is increased by ∼6-fold for the former and ∼20-fold for the latter. Consequently, the ratio between them decreases, approaching unity when the nanojunction is highly stressed. The implications are two-fold: On one hand, this means that mechanically stressing the nanojunction does not favor the (electro)mechanical switching mechanism. On the other hand, because the conductance of each individual species can be modulated by means of an external force, the system can also be used as a mechanically triggered switch.

Our findings are rationalized in terms of the changes in the electronic structure of the system as a function of the mechanical stretching of the molecular nanojunction.

METHODOLOGY

All calculations were performed using the density functional theory (DFT) code SIESTA.[40] Exchange and correlation effects were taken into account using the generalized gradient approximation within the Perdew−Burke−Ernzerhof (PBE) formalism.[41] Norm-conserving pseudopotentials (with relativistic corrections in the case of Au) generated according to the scheme of Troullier and Martins[42,43] were used. The separation between the periodic images was always maintained at 15 Å in all directions to ensure no interaction between them. The calculations were performed using the Γ point of the Brillouin zone and a double-ζ basis set with polarization. The energy shift used to confine the electrons in the pseudoatomic orbitals was 10 meV, and for the energy cutoff that defines the grid used to represent the charge density, a value of 200 Ry (∼2.7 keV) was used. We took care to test the convergence of our results with respect to all of these parameters. Geometry optimizations were performed using the conjugate gradient (CG) algorithm until a maximum force of 0.01 eV/Å was reached.

The molecular switch under study consists of a 4,4′-biphenyldithiol molecule with a disulfide bridge between the 2 and 2′ carbon atoms. The molecule/metal hybrid junction is modeled by binding this molecular species to two 23-atom Au clusters. Further details about the building of the pyramidal Au clusters and the initial structures for the molecular junction can be found elsewhere.[39] When the disulfide bridge is closed (i.e., when it is oxidized), the torsion angle between the rings is constrained to a value of ∼30°. This constitutes the high-conductance species, labeled henceforth as **Au−S−Ox**. On the other hand, when the disulfide bridge is opened by a reduction reaction, the low-conductance species (**Au−S−Red**) is obtained. Two different binding geometries to the Au clusters were considered: cis, in which both terminal thiol groups are appended to the gold clusters on the same side with respect to both Au clusters, and trans, in which the thiol groups are appended on opposite sides of the gold clusters. The mechanical properties of cis and trans **Au−S−Ox** were studied by means of a series of constrained geometry optimizations, and the results were already reported in ref 39. For both cis and trans **Au−S−Ox**, the energy profile along the stretching pathway displays a sawtooth-like behavior with three well-defined minima before the final breakage. The structures corresponding to these minima, at stretching distances (d) of 0.4 Å (0.2 Å), 2.7 Å (2.7 Å), and 5.6 Å (5.7 Å), for the cis (trans) geometry, were selected for this work in order to study the thermodynamics of the reduction reactions and the transport properties of the species involved.

The thermodynamics of the reduction reactions on both sulfur sites (anchoring and disulfide bridge) were studied. Hydrogen atoms were added at suitable positions close to the sulfur atoms of either the anchoring sites or the disulfide bridge. A subsequent geometry optimization was performed for each structure. The reduction of the disulfide bridge yields the aforementioned low-conductance species, **Au−S−Red**. The reduction of the anchoring S atoms, on the other hand, gives an undesired byproduct (termed as such because of its lower stability) that is denoted henceforth as **Au−SH−Ox**. The molecular structures of all the species involved in this study are illustrated in Scheme 1.

An in-house code based on the nonequilibrium Green's function (NEGF) operator[44] was employed to calculate the transport properties of **Au−S−Ox** and **Au−S−Red** at selected stretching distances along the pulling pathways for the cis and trans geometries. The implementation of the code was discussed in detail elsewhere.[45] As described in ref 39, the SIESTA Hamiltonian was used, considering that all s, p, and d Au pseudo-orbitals are equally coupled to the leads through the parameter $\gamma = -2.82$ eV. In the present work, a total of 24 leads were used to contact the Au atoms in the outermost planes of the clusters.

RESULTS AND DISCUSSION

As mentioned in the previous section, the mechanical stretching pathway of **Au−S−Ox** was already reported in our previous work.[39] There, it was shown that this metal/molecule hybrid nanojunction can be stretched by ∼8.5 Å before it finally breaks. A series of elastic and plastic deformations of the nanojunction were observed. Each of the three elastic regions is characterized by a well-defined minimum. Plastic deformation upon stretching involves abrupt changes in the bonding of the molecule to the metallic clusters. The results reported in ref 39 on the thermodynamics of the reduction reaction and the transport properties of the species involved were based on the first minimum encountered along the stretching pathway.

The present work evaluates the effects of mechanical pulling on two of the key properties of the molecular switch: first, the thermodynamics of the reduction reaction leading to **Au−S−Red** or **Au−SH−Ox** and, second, the electron-transport properties of the high- and low-conductance species of the molecular switch. These calculations involve structures that

DOI: 10.1021/jp510697a
J. Phys. Chem. C XXXX, XXX, XXX−XXX

correspond to the other two minima along the stretching pathway.

We note in passing that these particular geometries were taken to be illustrative for each elastic deformation region, and it was assumed that the calculated properties would change continuously between them.

The corresponding results are presented and discussed in two separate sections.

Thermodynamics of the Switching Reaction. As already pointed out, the (electro)chemical activation of the molecular switch involves the reduction of the disulfide bridge in **Au−S−Ox**. This yields **Au−S−Red** as a product. A potential reduction byproduct, **Au−SH−Ox**, that originates from reducing the anchoring S atoms was also considered. To evaluate the influence of mechanically stretching the molecular junction on the thermodynamics of these reactions, the corresponding energy changes, ΔU_{red}, given by

$$\Delta U_{red} = E(\textbf{Au−S−Red or Au−SH−Ox}) - E(\textbf{Au−S−Ox}) - E(H_2) \quad (1)$$

were calculated for selected structures along the stretching pathways of cis and trans **Au−S−Ox**. The corresponding results are summarized in Table 1.

Table 1. Energy of Reaction (ΔU_{red}) for the Reduction of Bridge and Anchoring Sulfur Atoms of Cis and Trans Au−S−Ox

stretching distance (Å)	ΔU_{red} (bridge) (eV)	ΔU_{red} (anchoring) (eV)	$\Delta\Delta U_{red}$[a] (anchoring bridge) (eV)	$\Delta\Delta U_{red}^{corr}$[b]
		cis **Au−S−Ox**		
0.4[c]	−0.426	0.163	0.589	0.607
2.7[d]	−0.503	0.097	0.600	0.601
5.6[d]	−0.366	−0.107	0.259	0.347
		trans **Au−S−Ox**		
0.2[c]	−0.384	0.266	0.650	0.823
2.7[d]	−0.528	0.081	0.609	0.699
5.7[d]	−0.358	−0.046	0.312	0.358

[a]Calculated from total electronic energies only. [b]Values corrected by adding enthalpic and entropic vibrational contributions obtained from normal-mode analysis (see Supporting Information for more details). [c]Values taken from ref 39. [d]This work.

No substantial differences exist between the cis and trans configurations. The reduction of the disulfide bridge is *always* more favorable than that of the anchoring sulfur atoms, which is the desired behavior for the application of the present molecular junction as a switch. Interestingly, the mechanical stress has a greater effect on the reduction on the anchoring S atoms than on those of the disulfide bridge. In this way, the thermodynamics of the switching reaction is not greatly affected, but the ratio between the possible products is modified in such a way that the undesired byproduct is relatively more favored at large stretching distances. It should be noted that the total stretching distance for both the cis and trans configurations up to rupture is ∼9.0 Å.[39] At low and medium stretching distances (up to ∼5.5 Å), the energy difference for the two reduction reactions ($\Delta\Delta U_{red}$) is ∼0.6 eV, but for relatively high stretching distances (>5.6 Å for the cis configuration and >5.7 Å for the trans configuration), this difference is reduced to ∼0.3 eV (a reduction of ca. 50%).

This effect of the stretching distance on the ratio between the two possible products can be traced to a relative *destabilization* of the product of the reduction on the disulfide bridge with respect to the product obtained by reduction of the anchoring sulfur atoms. The vibrational contributions to the enthalpic and entropic terms were calculated from the normal-mode analysis of both reduction products. The thermodynamic ratios ($\Delta\Delta U_{red}$) were thus corrected, but these values were not significantly affected (more details in the Supporting Information).

The top panel in Figure 1 illustrates the relative variation of the energies of the reactant and products for selected structures

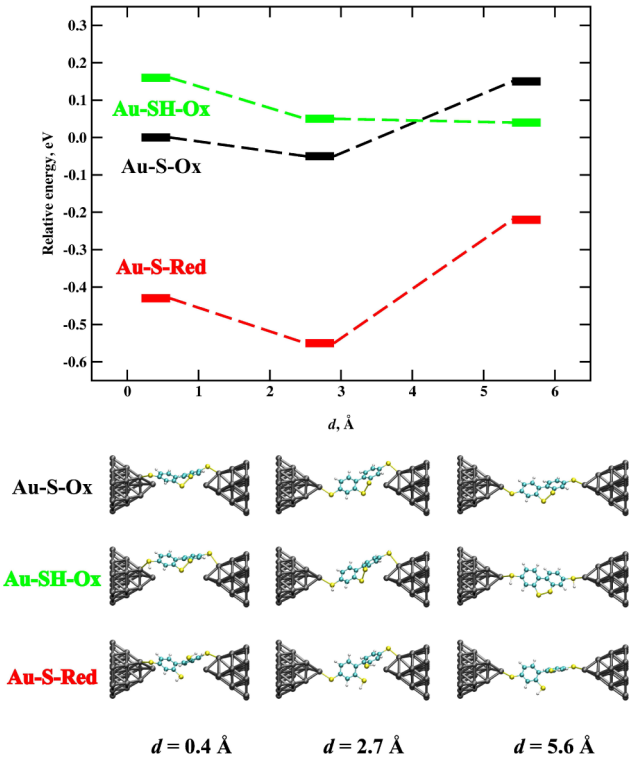

Figure 1. Top panel: Relative energies for the reactant (**Au−S−Ox**) and the two reduced products, at the disulfide bridge (**Au−S−Red**) and at the anchoring sulfur atoms (**Au−SH−Ox**), at selected distances (d) along the stretching pathway of cis **Au−S−Ox**. The reactant at d = 0.4 Å was taken as the reference. Bottom panel: Structures of **Au−S−Ox**, **Au−S−Red**, and **Au−SH−Ox** at the selected d values.

along the stretching pathway of **Au−S−Ox** cis [a similar situation is found for the trans configuration, illustrated in Figure S1 (Supporting Information)]. Two points are worthwhile noting: (i) From 0.4 to 2.7 Å, all species are slightly *stabilized* upon stretching, and the energy difference between the two reduced products is kept approximately constant. (ii) From 2.7 to 5.6 Å, **Au−S−Ox** and **Au−S−Red** are *destabilized* upon stretching, whereas the relative energy of **Au−SH−Ox** remains almost constant. This accounts for the reduction in $\Delta\Delta U_{red}$.

The relative stabilities of the two thiolated bound species (**Au−S−Ox** and **Au−S−Red**) are affected by the same factors upon stretching. This behavior can be rationalized in terms of the different bonding interactions between the molecular species considered with the Au leads. In our previous work,[39] we identified the relevance of a Au−C bonding interaction between the Au atoms in the apex of each cluster with a carbon

DOI: 10.1021/jp510697a
J. Phys. Chem. C XXXX, XXX, XXX−XXX

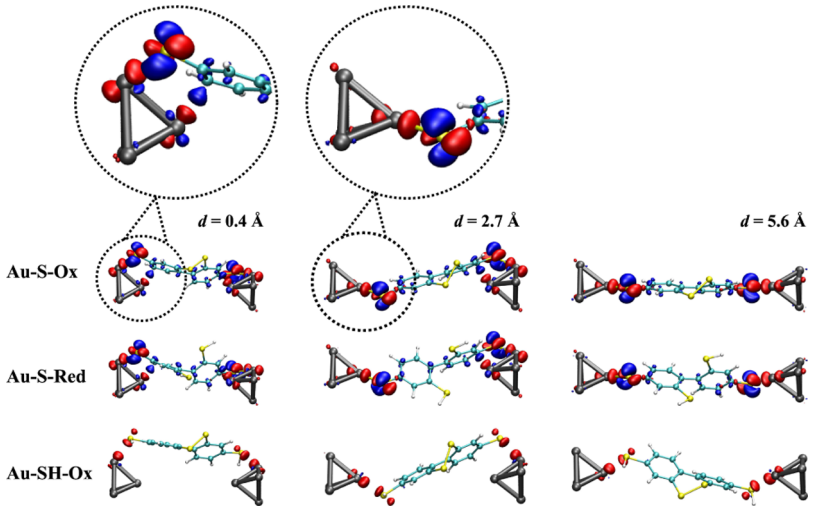

Figure 2. Calculated isosurface (at an isovalue of 0.005 e Bohr^{-3}) for the differential charge density at selected distances along the stretching pathway of cis **Au−S−Ox** and the reduction products on the sulfur anchoring atoms (**Au−SH−Ox**) and on the disulfide bridge (**Au−S−Red**). Note that some Au atoms from the clusters were omitted for clarity. Blue indicates a positive value (i.e., charge accumulation), and red indicates a negative value (i.e., charge depletion). The enlarged structures at the top for **Au−S−Ox** at d = 0.4 and 2.7 Å for one of the Au−S contacts allow a better visualization of the different bonding pattern in each case.

atom in each aromatic ring. This interaction was found to be relevant only for the thiolated bound species. When the anchoring sulfur atoms are reduced, this interaction is lost, mainly as a consequence of the longer Au−S bond distance. This Au−C interaction is of fundamental importance regarding the relative stability of **Au−S−Ox** and **Au−S−Red** along the stretching pathway. This issue was analyzed by means of the charge density differences between the different bonded molecular species and the combined isolated Au clusters and molecular radicals along the stretching pathway, as illustrated in Figure 2 for the cis geometry.

At d = 0.4 Å (0.2 Å) for the cis configuration [for the trans configuration, refer to Figure S2 (Supporting Information)], both S atoms are bonded to a Au atom on the edge of the pyramidal cluster. When the molecular junction is stretched, the main structural change regarding the Au−S bonding pattern is related to the breaking of this Au−S bond and the formation of a new Au−S bond with the atom in the apex of the cluster. This is observed, first, for one of the Au−S contacts (at d = 2.7 Å for both cis and trans configurations) and, after further stretching, for the other Au−S contact (at d = 5.6 Å for the cis configuration and d = 5.7 Å for the trans configuration). This is illustrated in the bottom panel of Figure 1. This modification in the bonding of the anchoring S atoms occurs concomitantly with the breaking of the Au−C interactions, as can be clearly appreciated in Figure 2. The relevant bonding interactions were also quantified in terms of the Mulliken overlap population (MOP) analysis[46] and are summarized in Table 2. For both thiolate bound species, the Au−C bonding interaction is gradually lost along the stretching pathway. On the other hand, the Au−S bonding interaction is slightly enhanced. This is due to a stronger interaction between the anchoring S atoms and the Au atoms in the apex of the cluster. This is also demonstrated by inspecting the projected density of states (pDOS) analysis of the corresponding atoms. The main bonding interactions are due to S 3p and Au 5d bands, as was shown to be case for the bonding of thiols to low-coordinated Au atoms on the surface of gold nanoparticles.[47] The structure of cis **Au−S−Ox** at d = 2.7 Å results an illustrative example, as one of the anchoring S atoms is bonded to the apex of the cluster, whereas the other is not. The dissected pDOS for each anchoring S atom is shown in Figure 3, where it can be appreciated that there is a better energy alignment between the S 3p and Au 5d bands of the S atom anchored to the apex Au atom. This is more evident around the Fermi level, where more well-defined common peaks can be observed in the latter case, in comparison to the S atom bonded to a more coordinated Au atom.

On the other hand, the electrostatic character of the bonding interaction between the molecular species with the gold leads does not change significantly along the stretching pathway, as demonstrated by the ΔQ values (charge transferred between the molecule and the gold clusters obtained from the corresponding Mulliken population analysis) compiled in Table 2. For **Au−S−Ox** and **Au−S−Red**, ∼0.4 e (e being the magnitude of the charge of an electron) is transferred from the gold clusters to the molecules. Values of ∼0.2 e have been reported in experimental[48−50] and theoretical[51,52] studies of alkyl thiols chemisorbed on gold surfaces.

This analysis shows that the main feature that affects the relative stability of the species involved in the switching reaction of the molecular junction studied is the breaking of a strong Au−C bonding interaction. This type of interaction is not unprecedented, as it was shown, by means of DFT calculations, that polycyclic aromatic hydrocarbons can interact with metallic surfaces.[53] It has also been shown that nonspecific van der Waals interactions between the molecule's backbone and the gold electrodes could play a significant role in the mechanical and the transport properties of the molecular junction.[54,55]

Transport Properties. Conductance values at zero bias (G/G_0, where G_0 is the quantum of conductance, $G_0 = 2e^2/h$ = 7.748×10^{-5}S) were calculated for the selected structures along the stretching pathways of cis and trans **Au−S−Ox** and the corresponding reduction product on the disulfide bridge (**Au−S−Red**). The results are summarized in Table 3. As pointed out in our previous work,[39] the fully oxidized species (**Au−S−Ox**) represents the closed state of the molecular switch and has

DOI: 10.1021/jp510697a
J. Phys. Chem. C XXXX, XXX, XXX−XXX

Table 2. Mulliken Population Analysis of the Anchoring Sulfur Atoms, Charge Transferred (ΔQ) from the Gold Clusters to the Molecule, and Mulliken Overlap Population (MOP) Analysis for the Au−C and Au−S Interactions for Selected Distances (d) Along the Pulling Pathways of Cis and Trans Au−S−Ox and Their Respective Reduction Products on the Sulfur Anchoring Atoms (Au−SH−Ox) and on the Disulfide Bridge (Au−S−Red)

				MOP (e)	
stretching distance (Å)		E_{frag}[a] (eV)	ΔQ[b] (e Au/molecule)	Au−S[c]	Au−C[d]
		cis **Au−S−Ox**			
0.4[e]	**Au−S−Ox**	4.00	+0.37/−0.37	0.22	0.10
	Au−S−Red	4.16	+0.32/−0.32	0.20	0.10
	Au−SH−Ox	0.72	−0.24/+0.24	0.09	0.00
2.7[f]	**Au−S−Ox**	3.73	+0.39/−0.39	0.24	0.05
	Au−S−Red	4.18	+0.37/−0.37	0.25	0.05
	Au−SH−Ox	0.85	−0.28/+0.28	0.10	0.00
5.6[f]	**Au−S−Ox**	3.34	+0.32/−0.32	0.24	0.00
	Au−S−Red	3.61	+0.35/−0.35	0.25	0.00
	Au−SH−Ox	0.88	−0.30/+0.30	0.10	0.00
		trans **Au−S−Ox**			
0.2[e]	**Au−S−Ox**	4.25	+0.35/−0.35	0.22	0.11
	Au−S−Red	4.48	+0.33/−0.33	0.22	0.11
	Au−SH−Ox	0.94	−0.28/+0.28	0.06	0.05
2.7[f]	**Au−S−Ox**	3.78	+0.40/−0.40	0.24	0.05
	Au−S−Red	4.02	+0.34/−0.34	0.24	0.05
	Au−SH−Ox	0.86	−0.27/+0.27	0.09	0.00
5.7[f]	**Au−S−Ox**	3.36	+0.32/−0.32	0.24	0.00
	Au−S−Red	3.62	+0.35/−0.35	0.26	0.00
	Au−SH−Ox	0.91	−0.31/+0.31	0.10	0.00

[a]Calculated as $E_{AB}^{frag} = E(A) + E(B) - E(AB)$, where AB is the optimized molecular junction, whereas A and B are the fragments (i.e., the Au cluster and the molecule without further relaxation). [b]Obtained by summing the Mulliken charges for the gold clusters and the molecule, respectively. [c]Obtained by summing the MOP contributions between the anchoring S atoms and all Au atoms of the cluster to which it is bonded. The values reported are the averages for the two anchoring S atoms in the molecule. [d]Obtained by summing the MOP contributions between the C atoms in each aromatic ring and all Au atoms of the nearest cluster. The values reported are the averages for both aromatic rings in the molecule. [e]Values taken from ref 39. [f]This work.

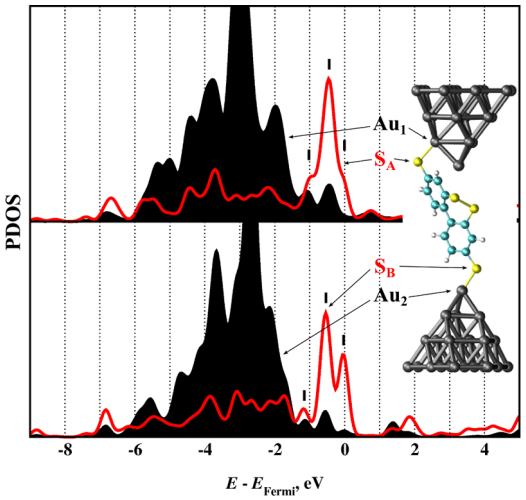

Figure 3. pDOS analysis for cis **Au−S−Ox** at d = 2.7 Å. The structure is shown as an inset. Top graph: Projected density of states for the S_A 3p (red line) and Au_1 5d (black shaded area) orbitals. Bottom graph: Projected density of states for the S_B 3p (red line) and Au_2 5d (black shaded area) orbitals. The labeling of the atoms corresponds to the illustration shown as an inset. The bands marked close to the Fermi level highlight the better energy alignment in the case of the Au_2−S_B bond.

a higher conductance than the opened state (**Au−S−Red**). It was also shown that, for both species, electron transport is dominated by the highest occupied molecular orbital (HOMO). The higher conductance of the closed state was attributed to the HOMO level being closer to the Fermi level of the nanojunction than the opened state. It should be noted that this *off-resonant* charge transport is in agreement with experimental and theoretical findings on other biphenyl molecules bonded to gold leads by means of Au−S bonds.[32,34]

Mechanical stretching of the molecular junction has a noticeable effect on the transport properties of the closed and opened forms of the molecular switch that is two-fold: On one hand, the absolute value of the conductance for both species *increases*, but on the other hand, the closed/opened ratio between the conductance values suffers a *decrease* from ∼3.0−7.0 when the molecular junction is compressed to ∼1.0 when it is stretched.

We are aware of the limitations of the DFT + NEGF scheme employed in this work, and thus, the conductance values reported in Table 3 should be not be regarded as quantitatively exact. Calculations based on the DFT + NEGF method are known to predict conductance values that are at least 1 order of magnitude larger than experimental data (see, for instance, refs 56−58 and references therein). This is mainly due to the fact that DFT underestimates the molecular HOMO−LUMO energy gap,[59] giving a higher density of states at the Fermi level and, thus, an overestimation of the conductance. Indeed, it has been shown that many-electron interactions are essential for accurately positioning frontier molecular orbital resonance energies in a junction.[60] Approximate methods have been proposed to improve DFT predictions such as the so-called DFT + Σ approach, in which self-energy corrections are introduced for the HOMO and LUMO energy levels based on experimental values.[56−58] This methodology has been shown to reproduce quantitatively experimental I−V characteristics in metal/molecule junctions.

Although the actual conductance values might not be quantitatively correct, comparing the ratios between the closed and opened species is more meaningful and should be well described beyond the errors introduced by the selected methodology.

The observed behavior can be traced to a shift in the HOMO for both the closed and the opened species to energies closer to the Fermi level as the pulling distance increases. This can be readily appreciated by examining the corresponding transmission curves, which are illustrated in Figure 4. The energies of the HOMOs relative to the Fermi level of the corresponding molecular junctions are summarized in Table 3. The trend observed confirms the results obtained from the transmission curves. Figure 5 shows the calculated isosurfaces for these orbitals. It can be observed that they all display a π symmetry and that this is not substantially altered along the stretching pathway.

DOI: 10.1021/jp510697a
J. Phys. Chem. C XXXX, XXX, XXX−XXX

Table 3. Conductance Values in Units of G_0 and Dihedral Angles between the Aromatic Rings at Selected Stretching Distances for Cis and Trans Au−S−Ox and the Respective Reduction Products on the Disulfide Bridge (Au−S−Red)

stretching distance (Å)		dihedral angle (deg)	$E - E_f$ (HOMO) (eV)	G/G_0	$G_{Au-S-Ox}/G_{Au-S-Red}$
		cis **Au−S−Ox**			
0.4	**Au−S−Ox**	25.5	−0.210	0.046	2.19
	Au−S−Red	54.7	−0.243	0.021	
2.7	**Au−S−Ox**	27.2	−0.061	0.295	3.14
	Au−S−Red	74.1	−0.077	0.094	
5.6	**Au−S−Ox**	25.1	−0.028	0.259	1.04
	Au−S−Red	64.3	−0.044	0.248	
		trans **Au−S−Ox**			
0.2	**Au−S−Ox**	33.5	−0.222	0.042	7.00
	Au−S−Red	68.1	−0.241	0.006	
2.7	**Au−S−Ox**	31.7	−0.117	0.197	1.03
	Au−S−Red	63.6	−0.064	0.192	
5.7	**Au−S−Ox**	27.1	−0.028	0.245	1.00
	Au−S−Red	63.9	−0.044	0.244	

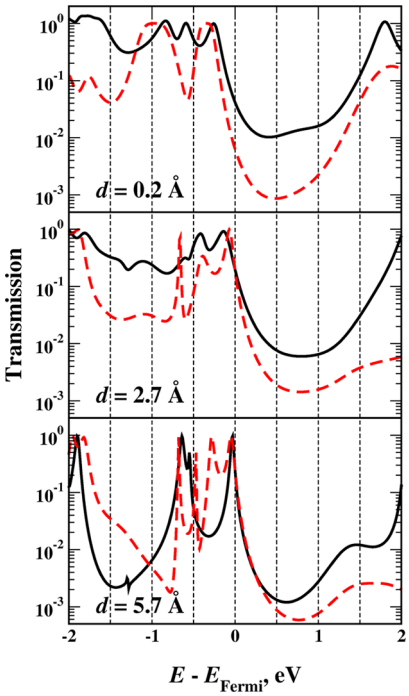

Figure 4. Transmission curves for **Au−S−Ox** (solid black lines) and **Au−S−Red** (dashed red lines) for the trans configuration.

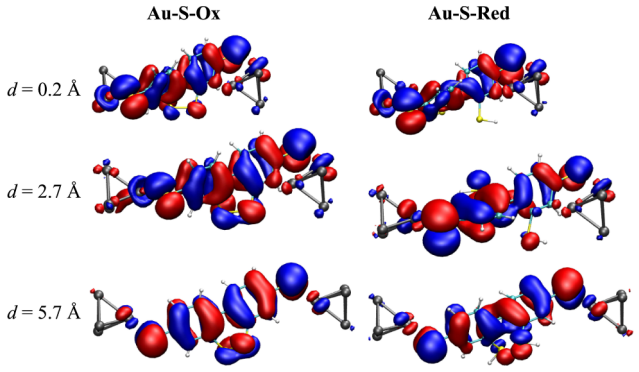

Figure 5. Calculated isosurfaces (at an isovalue of 0.05 e/Å^3) for the HOMOs of the trans **Au−S−Ox** system and the reduction product at the disulfide bridge (**Au−S−Red**) at selected distances (d) along the stretching pathway.

The effects on the transport properties can then be correlated with the structural changes along the stretching pathway. As already shown above, when the anchoring S atoms are bonded to the Au atom in the tip of the cluster, there is better overlap between the S 3p and Au 5d orbitals, and the bonding states lie closer to the Fermi level than when a S atom is bonded to the other Au atom (see Figure 3).

Interestingly, these results suggest that this system could be used as a molecular switch in two different ways: On one hand, the chemical activation of the disulfide bond allows the molecular junction to be switched between the high-conductance (closed) and low-conductance (opened) states. The highest conductance ratio occurs when the molecular junction is *compressed*. On the other hand, upon stretching of the molecular junction, this ratio is reduced, but the absolute conductance of each species increases, because of the structural modification in the anchoring pattern. It thus becomes possible to switch between low-conductance and high-conductance states by mechanically stretching the molecular junction with a ratio of ∼6 times for the fully oxidized species and ∼26 times for the structure that has been reduced at the disulfide bridge.

To further validate these results, an alternative procedure that would take into account the fluctuations caused by thermal motion would be desirable. A strategy similar to that employed in refs 45 and 55, namely, classical molecular dynamics with enhanced sampling and a Σ-extended Hückel hamiltonian + NEGF scheme for transport-property calculations, or the strategy employed in ref 14, which consists of a combination of ab initio molecular dynamics to obtain a statistically relevant sample of configurations and a DFT + NEGF approach to obtain the electrical conductance, would yield conductance histograms more comparable to those obtained experimentally.

CONCLUSIONS

We have shown that mechanical effects have a large effect on the proposed molecular switch. Stretching of the molecule/metal junction leads to significant structural changes that alter the bonding pattern of the molecule to the gold leads. This affects both the thermodynamics of the reduction reaction and the transport properties of the species involved. The former is affected in such a way that the ratio between the two possible products is reduced by ∼50%, favoring the undesired product in which the anchoring S atoms are reduced instead of those in the disulfide bridge. In contrast, for the latter, although the ratio

DOI: 10.1021/jp510697a
J. Phys. Chem. C XXXX, XXX, XXX−XXX

between the high- and low-conductance species of the molecular switch is dramatically reduced to ∼1, the absolute conductance of each individual species is greatly increased. This opens the possibility of a dual switching mechanism, namely, electrochemical and mechanical, for the system. The consideration of thermal motion and its effect on the transport properties of the system would be desirable. This would constitute a complete work on its own right and is clearly outside the scope of the present investigation, but it would be of interest in upcoming studies.

■ ASSOCIATED CONTENT

Supporting Information

Relative energies for the reactant (**Au−S−Ox**) and the two reduced products, at the disulfide bridge (**Au−S−Red**) and at the anchoring sulfur atoms (**Au−SH−Ox**), at selected distances (*d*) along the stretching pathway of trans **Au−S−Ox** (Figure S1). Calculated isosurface for the differential charge density at selected distances along the stretching pathway of trans **Au−S−Ox** and the corresponding reduction products (Figure S2). Transmission curves at different stretching distances for **Au−S−Ox** and **Au−S−Red** at the cis geometry (Figure S3). Detailed account of the normal-mode analysis and the calculation of the enthalpic and entropic vibrational contributions to the energy difference between the two reduction products. This material is available free of charge via the Internet at http://pubs.acs.org.

■ AUTHOR INFORMATION

Corresponding Author

*E-mail: martinz@fcq.unc.edu.ar. Phone: +54 0 351 5838383. Fax: +54 0 351 5838383.

Present Address

‡Lehrstuhl für Theoretische Chemie, Ruhr-Universität Bochum, 44801 Bochum, Germany.

Notes

The authors declare no competing financial interest.

■ ACKNOWLEDGMENTS

The authors acknowledge SECyT (Universidad Nacional de Córdoba), CONICET PIP 112-200801-000983 and PIP 11220110100992, Program BID (PICT 2012-2324), and PME 2006-01581 for financial support. M.E.C. is a grateful recipient of a Ph.D. scholarship from CONICET. The authors thank Dr. Christian F. A. Negre for providing the first version of the home-built NEGF code.

■ REFERENCES

(1) Xiang, D.; Jeong, H.; Lee, T.; Mayer, D. *Adv. Mater.* **2013**, *25*, 4845−4867.

(2) Walker, A. V. *J. Vac. Sci. Technol. A* **2013**, *31*, 050816.

(3) Son, J. Y.; Song, H. *Curr. Appl. Phys.* **2013**, *13*, 1157−1171.

(4) Aradhya, S. V.; Venkataraman, L. *Nat. Nanotechnol.* **2013**, *8*, 399−410.

(5) Arroyo, C. R.; Tarkuc, S.; Frisenda, R.; Seldenthuis, J. S.; Woerde, C. H. M.; Eelkema, R.; Grozema, F. C.; van der Zant, H. S. J. *Angew. Chem., Int. Ed.* **2013**, *52*, 3152−3155.

(6) Solomon, G. C.; Herrmann, C.; Ratner, M. A. In *Unimolecular and Supramolecular Electronics II*; Metzger, R. M., Ed.; Topics in Current Chemistry; Springer: Berlin, 2012; Vol. *313*, pp 1−38.

(7) Metzger, R. M.; Mattern, D. L. In *Unimolecular and Supramolecular Electronics II*; Metzger, R. M., Ed.; Topics in Current Chemistry; Springer: Berlin, 2012; Vol. *313*, pp 39−84.

(8) Li, C.; Mishchenko, A.; Wandlowski, T. In *Unimolecular and Supramolecular Electronics II*. Metzger, R. M., Ed.; Topics in Current Chemistry; Springer: Berlin, 2012; Vol. *313*, pp 121−188.

(9) Cuevas, J. C.; Scheer, E. *Molecular Electronics: An Introduction to Theory and Experiment*; World Scientific Publishing Co. Pte. Ltd.: Singapore, 2010.

(10) Tao, N. J. *Nat. Nanotechnol.* **2006**, *1*, 173−181.

(11) Zimbovskaya, N. A.; Pederson, M. R. *Phys. Rep.* **2011**, *509*, 1−87.

(12) Zoloff Michoff, M. E.; Vélez, P.; Dassie, S. A.; Leiva, E. P. M. In *Electrodeposited Nanowires and Their Applications*; Lupu, N., Ed.; InTech: Rijeka, Croatia, 2010; Chapter 1, pp 1−34.

(13) Taylor, J.; Guo, H.; Wang, J. *Phys. Rev. B* **2001**, *63*, 245407.

(14) Nguyen, H. C.; Szyja, B. M.; Doltsinis, N. L. *Phys. Rev. B* **2014**, *90*, 115440.

(15) Ribas-Arino, J.; Marx, D. *Chem. Rev.* **2012**, *112*, 5412−5487.

(16) Kim, Y.; Song, H.; Strigl, F.; Pernau, H.-F.; Lee, T.; Scheer, E. *Phys. Rev. Lett.* **2011**, *106*, 196804.

(17) Vélez, P.; Dassie, S. A.; Leiva, E. P. M. *Phys. Rev. B* **2010**, *81*, 235435.

(18) Michoff, M. E. Z.; Vélez, P.; Leiva, E. P. M. *J. Phys. Chem. C* **2009**, *113*, 3850−3854.

(19) Konôpka, M.; Turanský, R.; Dubecký, M.; Marx, D.; Štich, I. *J. Phys. Chem. C* **2009**, *113*, 8878−8887.

(20) Vélez, P.; Dassie, S.; Leiva, E. *Chem. Phys. Lett.* **2008**, *460*, 261−265.

(21) Vélez, P.; Dassie, S.; Leiva, E. P. M. *Phys. Rev. Lett.* **2005**, *95*, 045503.

(22) Konôpka, M.; Turanský, R.; Reichert, J.; Fuchs, H.; Marx, D.; Štich, I. *Phys. Rev. Lett.* **2008**, *100*, 115503.

(23) Krüger, D.; Fuchs, H.; Rousseau, R.; Marx, D.; Parrinello, M. *Phys. Rev. Lett.* **2002**, *89*, 186402.

(24) Franco, I.; Solomon, G. C.; Schatz, G. C.; Ratner, M. A. *J. Am. Chem. Soc.* **2011**, *133*, 15714−15720.

(25) Franco, I.; George, C. B.; Solomon, G. C.; Schatz, G. C.; Ratner, M. A. *J. Am. Chem. Soc.* **2011**, *133*, 2242−2249.

(26) Szyja, B. M.; Nguyen, H. C.; Kosov, D.; Doltsinis, N. L. *J. Mol. Model.* **2013**, *19*, 4173−4180.

(27) Lafferentz, L.; Ample, F.; Yu, H.; Hecht, S.; Joachim, C.; Grill, L. *Science* **2009**, *323*, 1193−1197.

(28) Li, Y.; Yin, Z.; Yao, J.; Zhao, J. *Chem. Lett.* **2009**, *38*, 334−335.

(29) Zhou, J.; Guo, C.; Xu, B. *J. Phys.: Condens. Matter* **2012**, *24*, 164209.

(30) Quek, S. Y.; Kamenetska, M.; Steigerwald, M. L.; Choi, H. J.; Louie, S. G.; Hybertsen, M. S.; Neaton, J. B.; Venkataraman, L. *Nat. Nanotechnol.* **2009**, *4*, 230−234.

(31) Chang, S.; He, J.; Kibel, A.; Lee, M.; Sankey, O.; Zhang, P.; Lindsay, S. *Nat. Nanotechnol.* **2009**, *4*, 297−301.

(32) Mishchenko, A.; Vonlanthen, D.; Meded, V.; Bürkle, M.; Li, C.; Pobelov, I. V.; Bagrets, A.; Viljas, J. K.; Pauly, F.; Evers, F.; Mayor, M.; Wandlowski, T. *Nano Lett.* **2010**, *10*, 156−163.

(33) Vonlanthen, D.; Mishchenko, A.; Elbing, M.; Neuburger, M.; Wandlowski, T.; Mayor, M. *Angew. Chem., Int. Ed.* **2009**, *48*, 8886−8890.

(34) Bürkle, M.; Viljas, J. K.; Vonlanthen, D.; Mishchenko, A.; Schön, G.; Mayor, M.; Wandlowski, T.; Pauly, F. *Phys. Rev. B* **2012**, *85*, 075417.

(35) Kondo, H.; Nara, J.; Kino, H.; Ohno, T. *J. Chem. Phys.* **2008**, *128*, 064701.

(36) Pauly, F.; Viljas, J. K.; Cuevas, J. C.; Schön, G. *Phys. Rev. B* **2008**, *77*, 155312.

(37) Sergueev, N.; Shin, S.; Kaviany, M.; Dunietz, B. *Phys. Rev. B* **2011**, *83*, 195415.

(38) Parker, S. M.; Smeu, M.; Franco, I.; Ratner, M. A.; Seideman, T. *Nano Lett.* **2014**, *14*, 4587−4591.

(39) Michoff, M. E. Z.; Castillo, M. E.; Leiva, E. P. M. *J. Phys. Chem. C* **2013**, *117*, 25724−25732.

DOI: 10.1021/jp510697a
J. Phys. Chem. C XXXX, XXX, XXX−XXX

(40) Soler, J. M.; Artacho, E.; Gale, J. D.; García, A.; Junquera, J.; Ordejón, P.; Sánchez-Portal, D. *J. Phys.: Condens. Matter* **2002**, *14*, 2745−2779.
(41) Perdew, J. P.; Burke, K.; Ernzerhof, M. *Phys. Rev. Lett.* **1996**, *77*, 3865−3868.
(42) Troullier, N.; Martins, J. L. *Phys. Rev. B* **1991**, *43*, 1993−2006.
(43) Troullier, N.; Martins, J. L. *Phys. Rev. B* **1991**, *43*, 8861−8869.
(44) Xue, Y.; Datta, S.; Ratner, M. A. *J. Chem. Phys.* **2001**, *115*, 4292−4299.
(45) Paz, S. A.; Zoloff Michoff, M. E.; Negre, C. F. A.; Olmos-Asar, J. A.; Mariscal, M. M.; Sánchez, C. G.; Leiva, E. P. M. *J. Chem. Theory Comput.* **2012**, *8*, 4539−4545.
(46) Mulliken, R. S. *J. Chem. Phys.* **1955**, *23*, 1841−1846.
(47) Jiang, D.-e.; Tiago, M. L.; Luo, W.; Dai, S. *J. Am. Chem. Soc.* **2008**, *130*, 2777−2779.
(48) Bourg, M.-C.; Badia, A.; Lennox, R. B. *J. Phys. Chem. B* **2000**, *104*, 6562−6567.
(49) Azzam, W.; Wehner, B. I.; Fischer, R. A.; Terfort, A.; Wöll, C. *Langmuir* **2002**, *18*, 7766−7769.
(50) Duwez, A.-S. *J. Electron Spectrosc.* **2004**, *134*, 97−138.
(51) Andreoni, W.; Curioni, A.; Grönbeck, H. *Int. J. Quantum Chem.* **2000**, *80*, 598−608.
(52) Franzen, S. *Chem. Phys. Lett.* **2003**, *381*, 315−321.
(53) Medeiros, P. V. C.; Gueorguiev, G. K.; Stafström, S. *Phys. Rev. B* **2012**, *85*, 205423.
(54) Aradhya, S. V.; Frei, M.; Hybertsen, M. S.; Venkataraman, L. *Nat. Mater.* **2012**, *11*, 872−876.
(55) Paz, S. A.; Michoff, M. E. Z.; Negre, C. F. A.; Olmos-Asar, J. A.; Mariscal, M. M.; Sánchez, C. G.; Leiva, E. P. M. *Phys. Chem. Chem. Phys.* **2013**, *15*, 1526−1531.
(56) Quek, S. Y.; Venkataraman, L.; Choi, H. J.; Louie, S. G.; Hybertsen, M. S.; Neaton, J. B. *Nano Lett.* **2007**, *7*, 3477−3482.
(57) Quek, S. Y.; Choi, H. J.; Louie, S. G.; Neaton, J. B. *Nano Lett.* **2009**, *9*, 3949−3953.
(58) Darancet, P.; Widawsky, J. R.; Choi, H. J.; Venkataraman, L.; Neaton, J. B. *Nano Lett.* **2012**, *12*, 6250−6254.
(59) Vélez, P.; Dassie, S. A.; Leiva, E. P. M. In *Recent Advances in Nanoscience*; Mariscal, M. M., Dassie, S. A., Eds., Research Signpost: Trivandrum-Kerala, India, 2007; pp 1−38.
(60) Neaton, J.; Hybertsen, M.; Louie, S. *Phys. Rev. Lett.* **2006**, *97*, 216405.

DOI: 10.1021/jp510697a
J. Phys. Chem. C XXXX, XXX, XXX−XXX